Mendeleev Communications

Mendeleev Commun., 2025, **35**, 711–713

Efficient performance of the Pd_1Cu_n/Al_2O_3 catalyst in front-end acetylene hydrogenation

Igor S. Mashkovsky,*[a] Pavel V. Markov,[a] Galina N. Baeva,[a] Anastasia E. Vaulina,[a,b] Nadezhda S. Smirnova,[a] Dmitry P. Melnikov[a,c] and Alexander Yu. Stakheev[a]

[a] *N. D. Zelinsky Institute of Organic Chemistry, Russian Academy of Sciences, 119991 Moscow, Russian Federation. E-mail: im@ioc.ac.ru*
[b] *D. I. Mendeleev University of Chemical Technology of Russia, 125047 Moscow, Russian Federation*
[c] *National University of Oil and Gas 'Gubkin University', 119991 Moscow, Russian Federation*

DOI: 10.71267/mencom.7850

Single-atom Pd_1Cu_n/Al_2O_3 catalysts were studied in front-end acetylene hydrogenation. It was found that the selectivity to ethylene increases sharply as the Pd : Cu ratio changes from 1 : 1 to 1 : 10. Single-atom $PdCu/Al_2O_3$ catalysts demonstrate remarkable resistance to CO swings and retain high selectivity in its absence, which are crucial for industrial applications.

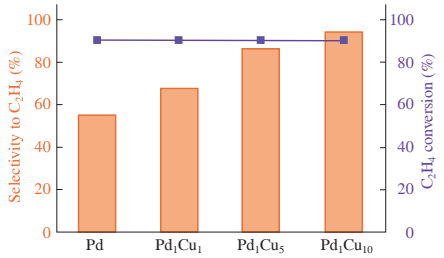

Keywords: acetylene hydrogenation, front-end, PdCu, single-atom catalyst, bimetallic alloy.

The ethylene obtained from naphtha cracking contains approximately 0.1 to 1% of acetylene by-products, which can disrupt Ziegler–Natta polymerization catalysts. To eliminate these traces of acetylene impurities, catalytic hydrogenation is a widely adopted technique in the industry.[1–5] Two common configurations can be used for acetylene hydrogenation. In the front-end configuration, the feed stream typically contains an excess of H_2 with an H_2/C_2H_2 ratio of up to 60–100. A negligible (<1%) amount of CO is also present in the feed as an inhibitor of C_2H_4 hydrogenation. In the tail-end configuration, a stoichiometric H_2/C_2H_2 ratio is usually employed. Compared to the tail-end configuration, the front-end configuration is significantly less studied.

In recent years, the PdM single-atom catalyst methodology has been successfully utilized in catalysis. A number of articles and reviews have been devoted to studying such catalysts in the selective hydrogenation of acetylenic compounds.[6–8] A significant increase in target selectivity has been demonstrated for PdAg,[9–12] PdAu,[13–15] PdCu,[16–19] and PdFe[20] systems. The authors attempted to determine specific structural and catalytic properties of single-atom systems and how they differ from classical bimetallic catalysts. For this purpose, the ratio of metals in the catalyst was varied over a wide range in order to eliminate multi-atomic Pd sites consisting of several atoms and to form Pd_1 single-atom sites isolated from each other by atoms of the 'inert' component. On the basis of the analysis of literature data, it was found that the modification of Pd with atoms from group 11 metals plays a key role in the synthesis of highly selective catalysts for the hydrogenation of acetylene compounds.[8]

This study examines the impact of the Pd : Cu ratio on the performance of the single-atom $PdCu/Al_2O_3$ catalyst in the front-end gas-phase hydrogenation. To the best of our knowledge, studies on the front-end hydrogenation of acetylene over PdCu-catalysts are extremely scarce.[18] All catalysts were obtained *via* incipient-wetness impregnation and characterized by transmission electron microscopy (TEM) and Fourier-transform infrared spectroscopy (FTIR-CO). For more experimental details, please see Online Supplementary Materials.

The morphology of the as-prepared Pd and PdCu samples was characterized using transmission electron microscopy (see Figure 1). The micrographs of all samples clearly show nearly spherical particles. The average particle size of the Pd/Al_2O_3 sample is 12.5 nm. The introduction of Cu results in a decrease in the average particle size. Thus, for the Pd_1Cu_1/Al_2O_3 sample, this value is ~10.6 nm. Further increasing the Pd : Cu ratio to 1 : 5

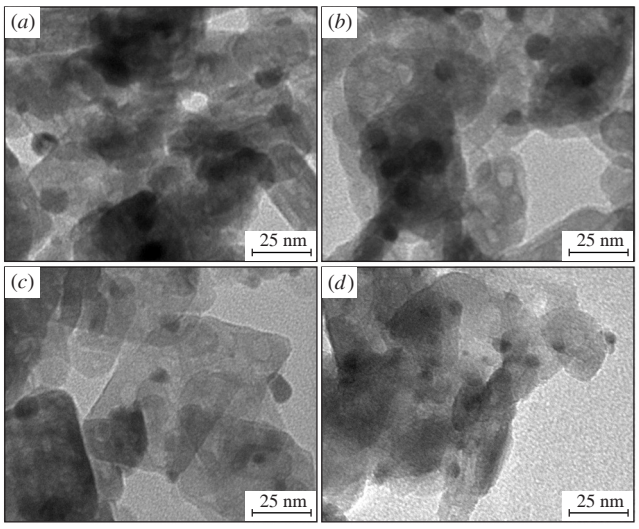

Figure 1 TEM micrographs of single-atom (*a*) Pd/Al_2O_3, (*b*) Pd_1Cu_1/Al_2O_3, (*c*) Pd_1Cu_5/Al_2O_3, and (*d*) Pd_1Cu_{10}/Al_2O_3 catalysts.

and 1 : 10 results in smaller particle sizes of ~7 nm for Pd_1Cu_5/Al_2O_3 and ~6.5 nm for Pd_1Cu_{10}/Al_2O_3. This trend has been observed previously for Pd–Cu catalysts indicating that the size of Pd–Cu bimetallic nanoparticles can be modified by adjusting the Cu content.[21,22] The authors attributed the decrease in particle size upon introduction of the Cu promoter to the formation of single-atom structures of active sites.

Figure 2 shows the CO-DRIFT spectra in the 2200–1800 cm^{-1} region for Pd/Al_2O_3, Cu/Al_2O_3, and $PdCu/Al_2O_3$ catalysts. The FTIR-CO spectrum of Pd/Al_2O_3 represents two broad absorption bands. The minor one centered at 2084 cm^{-1} is attributed to CO adsorbed linearly on palladium atoms, while a larger asymmetric band in the range of 2000–1800 cm^{-1} is ascribed to bridge-bonded and threefold CO. The peak centred at 1989 cm^{-1} is attributed to compressed-bridged CO species, while the shoulder at 1947 cm^{-1} belongs to isolated-bridged CO.[23] A small shoulder in the region of 1900–1800 cm^{-1} is indicative of CO adsorption on the threefold hollow Pd(111) site. The presence of bands below 2000 cm^{-1} indicates the presence of large palladium ensembles consisting of two or more adjacent Pd atoms, which serves as a hallmark of monometallic Pd.

The FTIR spectrum of adsorbed CO for the monometallic Cu/Al_2O_3 sample exhibits a broad infrared band centred at ~2120 cm^{-1} with a small shoulder at 2098 cm^{-1}. This band can be assigned to CO linearly bonded to Cu^+ in the Cu–Al–O system, while Cu^{2+}–CO carbonyls are usually observed in the range of 2220–2150 cm^{-1}.[24–26] The minor peak at ~2098 cm^{-1} is most likely attributed to Cu^0–CO surface carbonyls.[25,26] While the band near 2115 cm^{-1} is associated with Cu^0–CO species in ref. 27, two bands observed at 2115 and 2110 cm^{-1} in ref. 28 were ascribed to linearly adsorbed CO at Cu^+ and Cu^0 sites, respectively.

The DRIFT-CO spectrum of the Pd_1Cu_1/Al_2O_3 sample exhibits main CO adsorption bands at 2121, 2098, 2070, and 1989 cm^{-1}. Since no bands below 2100 cm^{-1} are exhibited by Cu, in the case of bimetallic $PdCu/Al_2O_3$ catalysts, the bands at lower wavenumbers can be clearly ascribed to CO adsorbed on palladium atoms.[28] The symmetric peak centred at 2070 cm^{-1} belongs to linearly adsorbed CO on Pd. The shift towards lower wavenumbers (2070 *vs.* 2084 cm^{-1} in Pd/Al_2O_3) indicates an interaction between Pd and Cu atoms, suggesting the formation of a bimetallic PdCu alloy. An intense band with a maximum at 1989 cm^{-1} has the same shape as in the FTIR-CO spectrum of Pd/Al_2O_3 and is related to bridge-bonded CO on Pd.

Adding Cu to Pd catalysts lowers the intensity of the bands corresponding to bridged and hollow-bonded CO, and/or shifts the peak wavenumbers.[29] Note that the enrichment of PdCu catalysts with copper leads to the complete disappearance of the absorption bands below 2000 cm^{-1}, while the bands corresponding to linearly bound CO on Pd (~2063–2064 cm^{-1}) are maintained. This indicates the presence of a surface structure wherein Pd atoms are separated from each other by Cu atoms, thereby forming isolated Pd_1 active sites. It has been previously shown that the single atom structure can be accomplished by substantial (atomic ratio of M : Pd ⩾ 40) dilution of palladium atoms by atoms of the host element.[18,19] Concurrently, evidence was presented demonstrating the formation of a single atom structure at a Cu : Pd ratio of 5.[30]

The results of the catalytic tests in the front-end acetylene hydrogenation are shown in Figures S1 and 3. As expected, the monometallic Pd catalyst exhibited the greatest activity (Figure S1). Acetylene conversion reached 99% at 92 °C. Adding copper insignificantly reduced the activity of all single-atom PdCu catalysts. Acetylene conversion reached 99% at 98 °C for Pd_1Cu_1/Al_2O_3, at 100 °C for Pd_1Cu_5/Al_2O_3, and at 101 °C for Pd_1Cu_{10}/Al_2O_3. The monometallic Cu catalyst had extremely low activity and was not included in the graph. Acetylene conversion reached only 12% at 212 °C.

The selectivity to ethylene also varied among the studied catalysts (Figure 3). Pd/Al_2O_3 exhibited the lowest selectivity, dropping to ~60% with acetylene conversion of ~88%. The single-atom Pd_1Cu_1/Al_2O_3 catalyst exhibited selectivity that was approximately 10% higher at comparable acetylene conversion (70 at 89%). Increasing the Cu content led to higher selectivity, reaching ~83% at acetylene conversion of 92% for Pd_1Cu_5/Al_2O_3 and ~93% at acetylene conversion of ~93% for Pd_1Cu_{10}/Al_2O_3. Note that the last two samples retained high selectivity at conversions exceeding 90%, including in the practically important range above 99%. This effect stems from the transformation of multiatomic Pd_n ($n > 2$) active sites into single-atom Pd_1 sites due to their isolation by the Cu one. This is confirmed by the DRIFTS-CO data. The generation of single-atom Pd_1 sites is evident in the complete disappearance of absorption bands below 2000 cm^{-1}, which are typical of bridged or multi-coordinated CO adsorption. The structure of the Pd_1 sites completely eliminates strong di-σ-bonded adsorption of the ethylene intermediate. Therefore, the transformation of monometallic Pd to Pd_1-containing species decreases the adsorption energy. Consequently, desorption from the catalyst surface is more favourable for the ethylene intermediate than overcoming the activation barrier of undesired hydrogenation into ethane.

CO is a potential inhibitor of the hydrogenation activity of precious metal catalysts. Therefore, its content in the feedstock

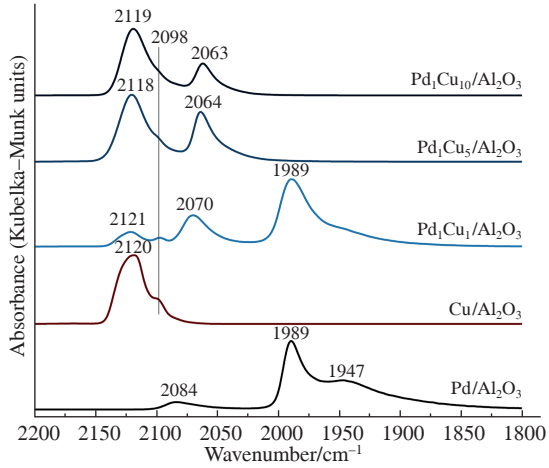

Figure 2 Normalized DRIFT-CO spectra for *in situ* reduced monometallic Pd/Al_2O_3 and Cu/Al_2O_3 and bimetallic $PdCu/Al_2O_3$ catalysts.

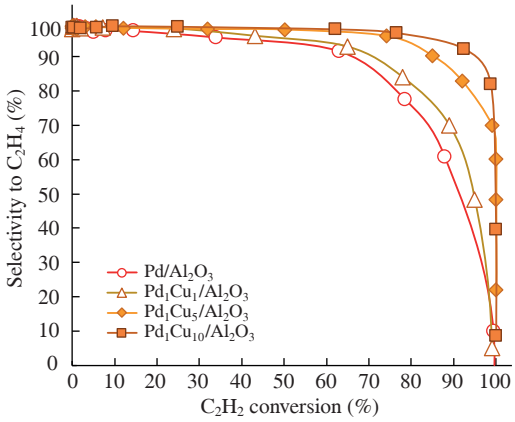

Figure 3 Dependence of C_2H_4 selectivity on C_2H_2 conversion for the Pd/Al_2O_3 and Pd_1Cu_n/Al_2O_3 catalysts in the front-end acetylene hydrogenation. For reaction conditions, please see Online Supplementary Materials.

is crucial to the stable operation of industrial front-end hydrogenation reactors. An important characteristic of front-end selective hydrogenation catalysts is how they respond to CO fluctuations in the feedstock. In industry, such swings are dangerous because a drop in CO could lead to uncontrolled hydrogenation of ethylene and temperature runaway.

To investigate the effect of CO under front-end conditions, additional tests were conducted without adding CO to the feedstock. Figure S2 shows the selectivity to ethylene at 90% acetylene conversion for the Pd/Al_2O_3 and $PdCu/Al_2O_3$ catalysts. For the Pd/Al_2O_3 catalyst, a CO drop-off led to a dramatic decrease in selectivity from 55% to –60% and, thus, to temperature runaway. The negative selectivity indicates that ethylene was largely involved in the reaction.[15,18,19] Bimetallic catalysts are less sensitive to CO swings. Under the same conditions, selectivity decreased from 68 to 40% for Pd_1Cu_1/Al_2O_3. The most stable was the Pd_1Cu_{10}/Al_2O_3 catalyst whose selectivity decreased from 94 to 86%. It can be concluded that the addition of Cu increases both the ethylene selectivity under front-end hydrogenation conditions and the stability to CO fluctuations in the feedstock.

Strong influence of CO on selectivity may be attributed to its strong adsorption on active sites with bridged-CO adsorption, which are associated with low selectivity. Under steady-state reaction conditions, the adsorption quasi-equilibrium 'turns off' the multi-point active sites that contribute to low ethylene selectivity. For bimetallic catalysts with a significantly lower concentration of these sites, this effect is less pronounced. This is particularly evident with the Pd_1Cu_{10}/Al_2O_3 catalyst, for which the selectivity increased by 8%. According to DRIFT-CO spectroscopy, the characteristic bands of multi-point adsorption are undetectable on the surface of this catalyst, confirming single-atom structure formation.

Several trends can be seen from the results of this study. Firstly, it was observed for PdCu catalysts that the size of PdCu bimetallic nanoparticles could be effectively modified by adjusting the content of the Cu counterpart. Secondly, the FTIR-CO data revealed that enrichment of the Pd catalyst with Cu in Pd:Cu molar ratios $\geqslant 1:5$ can be sufficient to form a surface single-atom structure, thereby providing excellent selectivity towards ethylene in the front-end acetylene hydrogenation reaction. Thirdly, as the Pd : Cu ratio increases, catalysts' activity in the front-end selective hydrogenation of acetylene decreases insignificantly while the selectivity to ethylene increases sharply. In addition, single-atom $PdCu/Al_2O_3$ catalysts exhibit remarkable resistance to CO swings and maintain selectivity in its absence, which is crucial for industrial applications.

This work was supported by the Russian Science Foundation (grant no. 23-13-00301, https://rscf.ru/en/project/23-13-00301). Electron microscopy characterization was performed in the Department of Structural Studies of Zelinsky Institute of Organic Chemistry, Moscow.

Online Supplementary Materials

Supplementary data associated with this article can be found in the online version at doi: 10.71267/mencom.7850.

References

1 M. T. Ravanchi, S. Sahebdelfar and S. Komeili, *Rev. Chem. Eng.*, 2018, **34**, 215; https://doi.org/10.1515/revce-2016-0036.
2 V. I. Bogdan, A. E. Koklin, A. N. Kalenchuk and L. M. Kustov, *Mendeleev Commun.*, 2020, **30**, 462; https://doi.org/10.1016/j.mencom.2020.07.018.
3 A. A. Shesterkina, L. M. Kozlova, I. V. Mishin, O. P. Tkachenko, G. I. Kapustin, V. P. Zakharov, M. S. Vlaskin, A. Z. Zhuk, O. A. Kirichenko and L. M. Kustov, *Mendeleev Commun.*, 2019, **29**, 339; https://doi.org/10.1016/j.mencom.2019.05.034.
4 H. Zea, K. Lester, A. K. Datye, E. Rightor, R. Gulotty, W. Waterman and M. Smith, *Appl. Catal., A*, 2005, **282**, 237; https://doi.org/10.1016/j.apcata.2004.12.026.
5 N. S. Schbib, M. A. García, C. E. Gígola and A. F. Errazu, *Ind. Eng. Chem. Res.*, 1996, **35**, 1496; https://doi.org/10.1021/ie950600k.
6 Y. Pan, X. Zhang, G. Sun, Y. Li and B. Liu, *ACS Catal.*, 2025, **15**, 3674; https://doi.org/10.1021/acscatal.4c08075.
7 X. Cao, B. W.-L. Jang, J. Hu, L. Wang and S. Zhang, *Molecules*, 2023, **28**, 2572; https://doi.org/10.3390/molecules28062572.
8 I. S. Mashkovsky, P. V. Markov, A. V. Rassolov, E. D. Patil and A. Yu. Stakheev, *Russ. Chem. Rev.*, 2023, **92**, RCR5087; https://doi.org/10.59761/RCR5087.
9 D. A. Shlyapin, D. V. Yurpalova, T. N. Afonasenko, V. L. Temerev and A. V. Lavrenov, *Catal. Ind.*, 2024, **16**, 278; https://doi.org/10.1134/S2070050424700156.
10 D. V. Glyzdova, N. S. Smirnova, D. A. Shlyapin and P. G. Tsyrul'nikov, *Russ. J. Gen. Chem.*, 2020, **90**, 1120; https://doi.org/10.1134/S1070363220060298.
11 I. S. Mashkovsky, A. V. Bukhtiyarov, P. V. Markov, G. O. Bragina, G. N. Baeva, N. S. Smirnova, M. A. Panafidin, I. A. Chetyrin, E. Yu. Gerasimov, Y. V. Zubavichus and A. Yu. Stakheev, *Appl. Surf. Sci.*, 2025, **681**, 161516; https://doi.org/10.1016/j.apsusc.2024.161516.
12 P. V. Markov, I. S. Mashkovsky, G. N. Baeva, D. P. Melnikov and A. Yu. Stakheev, *Mendeleev Commun.*, 2023, **33**, 836; https://doi.org/10.1016/j.mencom.2023.10.032.
13 J. Liu, J. Shan, F. R. Lucci, S. Cao, E. C. H. Sykes and M. Flytzani-Stephanopoulos, *Catal. Sci. Technol.*, 2017, **7**, 4276; https://doi.org/10.1039/C7CY00794A.
14 J. Ballesteros-Soberanas, N. Martín, M. Bacic, E. Tiburcio, M. Mon, J. C. Hernández-Garrido, C. Marini, M. Boronat, J. Ferrando-Soria, D. Armentano, E. Pardo and A. Leyva-Pérez, *Nat. Catal.*, 2024, **7**, 452; https://doi.org/10.1038/s41929-024-01130-7.
15 I. S. Mashkovsky, N. S. Smirnova, P. V. Markov, G. N. Baeva, A. E. Vaulina, D. P. Melnikov and A. Yu. Stakheev, *Mendeleev Commun.*, 2024, **34**, 718; https://doi.org/10.1016/j.mencom.2024.09.030.
16 F. Qin and W. Chen, *Chem. Commun.*, 2021, **57**, 2710; https://doi.org/10.1039/d1cc00062d.
17 F. Huang, M. Peng, Y. Chen, X. Cai, X. Qin, N. Wang, D. Xiao, L. Jin, G. Wang, X.-D. Wen, H. Liu and D. Ma, *J. Am. Chem. Soc.*, 2022, **144**, 18485; https://doi.org/10.1021/jacs.2c07208.
18 G. X. Pei, X. Y. Liu, X. Yang, L. Zhang, A. Wang, L. Li, H. Wang, X. Wang and T. Zhang, *ACS Catal.*, 2017, **7**, 1491; https://doi.org/10.1021/acscatal.6b03293.
19 G. Pei, X. Liu, M. Chai, A. Wang and T. Zhang, *Chin. J. Catal.*, 2017, **38**, 1540; https://doi.org/10.1016/S1872-2067(17)62847-X.
20 Z. Sun, C. Li, J. Lin, T. Guo, S. Song, Y. Hu, Z. Zhang, W. Yan, Y. Wang, Z. Wei, F. Zhang, K. Zheng, D. Wang, Z. Li, S. Wang and W. Chen, *ACS Nano*, 2024, **18**, 13286; https://doi.org/10.1021/acsnano.4c02710.
21 B. Yan, C. Wang, H. Xu, K. Zhang, S. Li and Y. Du, *ChemPlusChem*, 2017, **82**, 1121; https://doi.org/10.1002/cplu.201700245.
22 A. V. Rassolov, G. N. Baeva, I. S. Mashkovsky and A. Yu. Stakheev, *Mendeleev Commun.*, 2018, **28**, 538; https://doi.org/10.1016/j.mencom.2018.09.030.
23 S. K. Kim, C. Kim, J. H. Lee, J. Kim, H. Lee and S. H. Moon, *J. Catal.*, 2013, **306**, 146; https://doi.org/10.1016/j.jcat.2013.06.018.
24 J. Sá, S. Gross and H. Vinek, *Appl. Catal. A*, 2005, **294**, 226; https://doi.org/10.1016/j.apcata.2005.07.046.
25 M. B. Padley, C. H. Rochester, G. J. Hutchings and F. King, *J. Catal.*, 1994, **148**, 438; https://doi.org/10.1006/jcat.1994.1230.
26 K. I. Hadjiivanov and G. N. Vayssilov, *Adv. Catal.*, 2002, **47**, 307; https://doi.org/10.1016/0920-5861(95)00163-8.
27 B. T. Meshesha, N. Barrabés, J. Llorca, A. Dafinov, F. Medina and K. Föttinger, *Appl. Catal., A*, 2013, **453**, 130; https://doi.org/10.1016/j.apcata.2012.12.019.
28 A. J. McCue and J. A. Anderson, *J. Catal.*, 2015, **329**, 538; https://doi.org/10.1016/j.jcat.2015.06.002.
29 M. Lesiak, M. Binczarski, S. Karski, W. Maniukiewicz, J. Rogowski, E. Szubiakiewicz, J. Berlowska, P. Dziugan and I. Witońska, *J. Mol. Catal. A: Chem.*, 2014, **395**, 337; https://doi.org/10.1016/j.molcata.2014.08.041.
30 F. Xing, J. Jeon, T. Toyao, K. Shimizu and S. Furukawa, *Chem. Sci.*, 2019, **10**, 8292; https://doi.org/10.1039/C9SC03172C.

Received: 16th June 2025; Com. 25/7850